metals

Article

A Study on the Formation of Fiber Texture in the Subsurface Layer of Hot-Rolled Plate of 3.2%Si Grain-Oriented Steel

Xiang Zou *, Qingyou Liu and Shengtao Qiu

Central Iron and Steel Research Institute, Beijing 100081, China; qiust@cisri.com.cn (S.Q.)
* Correspondence: zou0919@hotmail.com

Abstract: During the hot rolling process, inhomogeneity microstructure and variations of texture along the thickness direction of hot-rolled plate were formed through shear deformation and recrystallization. The purpose of this study is to investigate the formation and evolution of fiber texture in hot-rolled plate of grain-oriented silicon steel. The results indicate that, in the surface layer s = 1 of hot-rolled plate, a large number of equiaxed grains are formed under high shear force. Under the surface layer, as shear force gradually decreases along the thickness direction, the grain aspect ratio of recrystallized grains gradually increases along the thickness direction of hot-rolled plate, and the shape of the recrystallized grains formed in the subsurface layer and center layer becomes more irregular along the thickness direction. Under the combination of compressive force and decreasing shear force along the thickness direction, fiber texture composed of dozens of specific orientations (such as {112}<111>, {110}<112>, {213}<364>, {441}<104> and Goss orientations) is formed in the subsurface layer s = 0.5~0.9 and gradually evolves along the thickness direction. Therefore, the formation of Goss texture is a small part of fiber texture and is the result of texture evolution in the subsurface layer s = 0.5~0.9.

Keywords: grain-oriented silicon steel; shear force; inhomogeneous microstructure; fiber texture; Goss texture

Citation: Zou, X.; Liu, Q.; Qiu, S. A Study on the Formation of Fiber Texture in the Subsurface Layer of Hot-Rolled Plate of 3.2%Si Grain-Oriented Steel. *Metals* **2023**, *13*, 1597. https://doi.org/10.3390/met13091597

Academic Editor: Zbigniew Pater

Received: 17 August 2023
Revised: 4 September 2023
Accepted: 13 September 2023
Published: 15 September 2023

1. Introduction

Grain-oriented silicon steel has been widely used as a soft magnetic material in the power industry; the sharpness of secondary recrystallization Goss texture [1,2] determines the magnetic properties of grain-oriented silicon steel [3]. Goss texture has always been a major research subject of grain-oriented silicon steel, and researchers have proposed some hypotheses about the origin of Goss nuclei and made significant progress in studying the formation of Goss-oriented grains during hot rolling. However, the formation and evolution of texture [4,5] during hot rolling [6] is still an important and interesting research field in the manufacturing process [7] of grain-oriented silicon steel [8,9].

Forty-eight slip systems exist in the BCC (body-centered cubic) metals. Constrained by the initial orientation and Schmid factor, only several specific slip systems can be activated in the rolling process, which contributes to the formation of preferred orientations [10] and variations of rolling texture [11]. During the hot rolling process, the hot roller applies shear force parallel to the rolling direction and compressive force parallel to the normal direction to the hot-rolled plate. Mukhopadhyay [12] reported that shear strain decreased along the thickness of the hot-rolled plate during hot rolling. The shear force parallel to the rolling direction had a maximum value near the surface layer of hot-rolled plate and decreased along the thickness direction, eventually decreasing to nearly zero in the center layer, while the compressive force parallel to the normal direction could be regarded as a constant during hot rolling.

Munetsugu [13,14] investigated the density of (110), (100) and (111) though the thickness of the hot-rolled sheet and proposed that a texture gradient was formed in the hot-rolled sheet of 3%Si grain-oriented steel, and that Goss-oriented grains were formed in the intermediate layer through deformation and recrystallization during the hot rolling process. Inokuti et al. [15,16] reported that (110)[001] Goss grains were preferentially formed in specific areas of the hot-rolled plate, and the nuclei of Goss grains in the hot-rolled plate were subsequently preserved through the mechanism of "texture inheritance", resulting in the preferential growth [17] of Goss-oriented grains [18,19] during the secondary recrystallization process [20]. Bottcher [21] and Mishra [22] conducted detailed research on the distribution of α-fiber (<110>//RD), γ-fiber (<111>//ND) and η-fiber (<100>//RD) in the hot-rolled plate of grain-oriented silicon steel, and concluded that, due to the dispersive distribution of inhibitors [23] inhibiting the growth of normal grains [24], abnormal Goss grains grew at the expense of primary recrystallized grains and eventually developed a sharp Goss texture during secondary recrystallization. Bottcher [20] and Inokuti [25] also investigated the effect of the double-surface removal of the hot-rolled plate on grain-oriented electrical steel and reported that double-surface removal had a detrimental impact on the secondary recrystallization and magnetic properties of grain-oriented silicon steel. The amount of double-sided removal determined the reduction in magnetic properties, as the nuclei of Goss grains in the hot-rolled plate were not inherited, which could result in imperfect secondary recrystallization. Therefore, the formation and evolution of Goss texture in the hot-rolled plate are essential for obtaining the high permeability of grain-oriented electrical steel [26,27]. Jiang et al. [28] conducted a detailed study on three texture components ({110}<001>, {112}<111> and {110}<112> texture) in the surface layer of a 2.5%Si hot-rolled plate; however, {110}<001>, {112}<111> and {110}<112> textures only accounted for a portion of the texture of hot-rolled plate.

Previous studies have investigated α-fiber, γ-fiber and some independent texture components formed in the hot-rolled plate of grain-oriented silicon steel; however, the overall texture and other shear texture components in the hot-rolled plate have not yet been analyzed and discussed. This article investigates the formation and evolution of fiber texture composed of dozens of specific orientations in the subsurface layer of hot-rolled plate. The relationship between shear force and the formation of texture and microstructure in the hot-rolled plate of grain-oriented silicon steel is the focus of this study.

2. Materials and Methods

During hot rolling, a 240 mm slab manufactured through continuous casting was reheated to approximately 1140 °C, and then the 240 mm slab was rolled into a 40 mm rolled sheet through 5 passes (190 mm–145 mm–105 mm–70 mm–40 mm) of rough rolling, and the finishing temperature of rough rolling was approximately 1040 °C. The 40 mm rolled sheet was rolled into a 2.6 mm hot-rolled plate through 7 passes (22.4 mm–11.2 mm–6.8 mm–4.6 mm–3.6 mm–3.1 mm–2.6 mm) of finish rolling. The rolling mill was a four-high non-reversing rolling mill with a working roll diameter of 700 mm and a length of 2550 mm, and the finishing temperature of finish rolling was approximately 940 °C.

The chemical composition of hot-rolled plate is shown in Table 1, and the magnetic induction of the final product can reach B_8 = 1.89 T. Finally, 2.6 mm thick hot-rolled plate was cut into 20 × 15 mm specimens for X-ray diffraction (XRD, PANalytical Empyrean Series 2 (Malvern Panalytical, Almelo, The Netherlands)) and 10 × 8 mm specimens for the optical microscope (Zeiss Axio Scope A1 (Carl Zeiss AG, Jena, Germany)) and scanning electron microscope (JSM-7900F (JEOL, Tokyo, Japan)).

Table 1. Chemical composition of hot-rolled plate (wt%).

Si	C	Als	Mn	Cu	N	S
3.2	0.06	0.028	0.10	0.2	0.009	0.007

In order to study the macro-texture evolution of hot-rolled plate along the thickness direction, 20 × 15 mm specimens of hot-rolled plate were mechanically ground layer by layer from the surface layer s = 1 to center layer s = 0. The thickness layer of hot-rolled plate is defined by s = 2a/b; a represents the distance from the center layer and b represents the whole plate thickness, s = ±1 represents the surface layer and s = 0 represents the center layer. Then, the specimens of each thickness layer (s = 0~1) of hot-rolled plate were obtained and measured for XRD, and complete (100) pole figures and ODFs (orientation distribution functions) [29] along the thickness direction of hot-rolled plate were obtained. The 10 × 8 mm specimens of hot-rolled plate were mechanically ground, polished and electrolytic-corroded to investigate the microstructure morphology of hot-rolled plate. The microstructure of the longitudinal section of hot-rolled plate was observed using an optical microscope, and different layers (surface layer, subsurface layer and center layer) of hot-rolled plate were selected to study the morphological evolution along the thickness direction and were detected using a scanning electron microscope (JSM-7900F) for EBSD (electron backscatter diffraction). RD represents rolling direction, TD and ND represent transverse direction and normal direction, respectively.

3. Results

3.1. Inhomogeneous Microstructure and the Distribution of Pole Intensity in the Hot-Rolled Plate

Figure 1a indicates that the microstructure of surface layers (s = ±1) is composed of completely recrystallized grains. Under the surface layer, fiber structures parallel to the rolling direction appear and increase along the thickness direction. In the center layer, the majority of the microstructure is composed of fiber structure, and large recrystallized grains can be observed to elongate along the rolling direction. Figure 1b illustrates the distribution of (100), (110), (111) and (112) pole intensities along the thickness direction of hot-rolled plate measured using XRD. The (110) pole intensity is concentrated in the layer s = −0.5~−0.9 and s = 0.5~0.9 but is at a minimum in the layer s = −0.4~0.4. The (111) and (112) pole intensities are concentrated in the layer s = −0.4~0.4 and are relatively weak in layers s = −0.5~−1 and s = 0.5~1. However, the (100) pole intensity is highly concentrated in the layer s = −0.4~0.4 and reaches a peak in the layer s = 0, but is weak in layers s = −0.5~−1 and s = 0.5~1. Therefore, according to texture type and morphology, s = −1 and s = 1 represent the surface layer of hot-rolled plate, s = −0.5~−0.9 and s = 0.5~0.9 represent the subsurface layer and s = −0.4~0.4 represents the center layer.

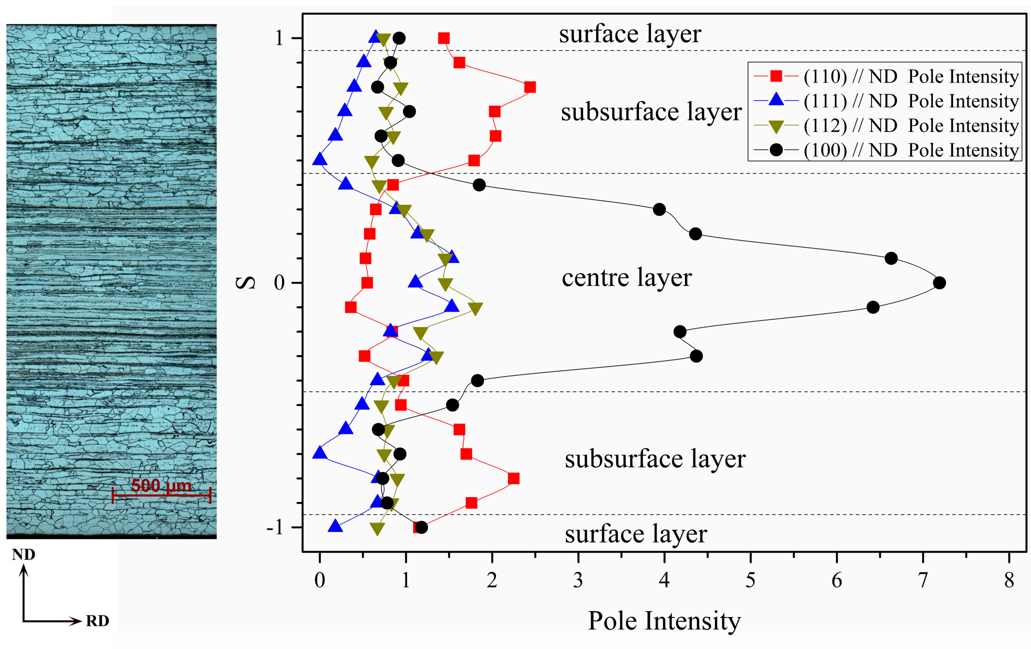

Figure 1. (**a**) The microstructure of longitudinal section of hot-rolled plate; (**b**) the distribution of (100), (110), (111) and (112) pole intensities along the thickness.

Figure 2 shows the grain aspect ratio of different layers of hot-rolled plate measured using EBSD, indicating that the recrystallized grain size gradually increases along the thickness direction, and some large grains in the center layer s = 0 can exceed 200 µm. The horizontal scale in Figure 2 represents grain aspect ratio (minimum value: 1, maximum value: 9), and the corresponding color of the grains represents the value of the grain aspect ratio. Figure 3 shows the comparison of the grain aspect ratio between different layers of hot-rolled plate. The microstructure of the surface layer s = 1 is mainly composed of equiaxed grains (Figure 2a), and the proportion of equiaxed grains with a grain aspect ratio of 1.0~2.0 is higher than that of the subsurface and center layers. Compared with the surface layer s = 1, the grain aspect ratio of recrystallized grains gradually increases in the subsurface layer s = 0.8, s = 0.5 and the center layer s = 0. Some recrystallized grains in the center layer s = 0 (Figure 2d) have a high grain aspect ratio of 4.0~9.0 and are significantly elongated along the rolling direction. Therefore, it is concluded that, along the thickness direction of hot-rolled plate, the shape of the recrystallized grains gradually elongates along the rolling direction and tends to be irregular.

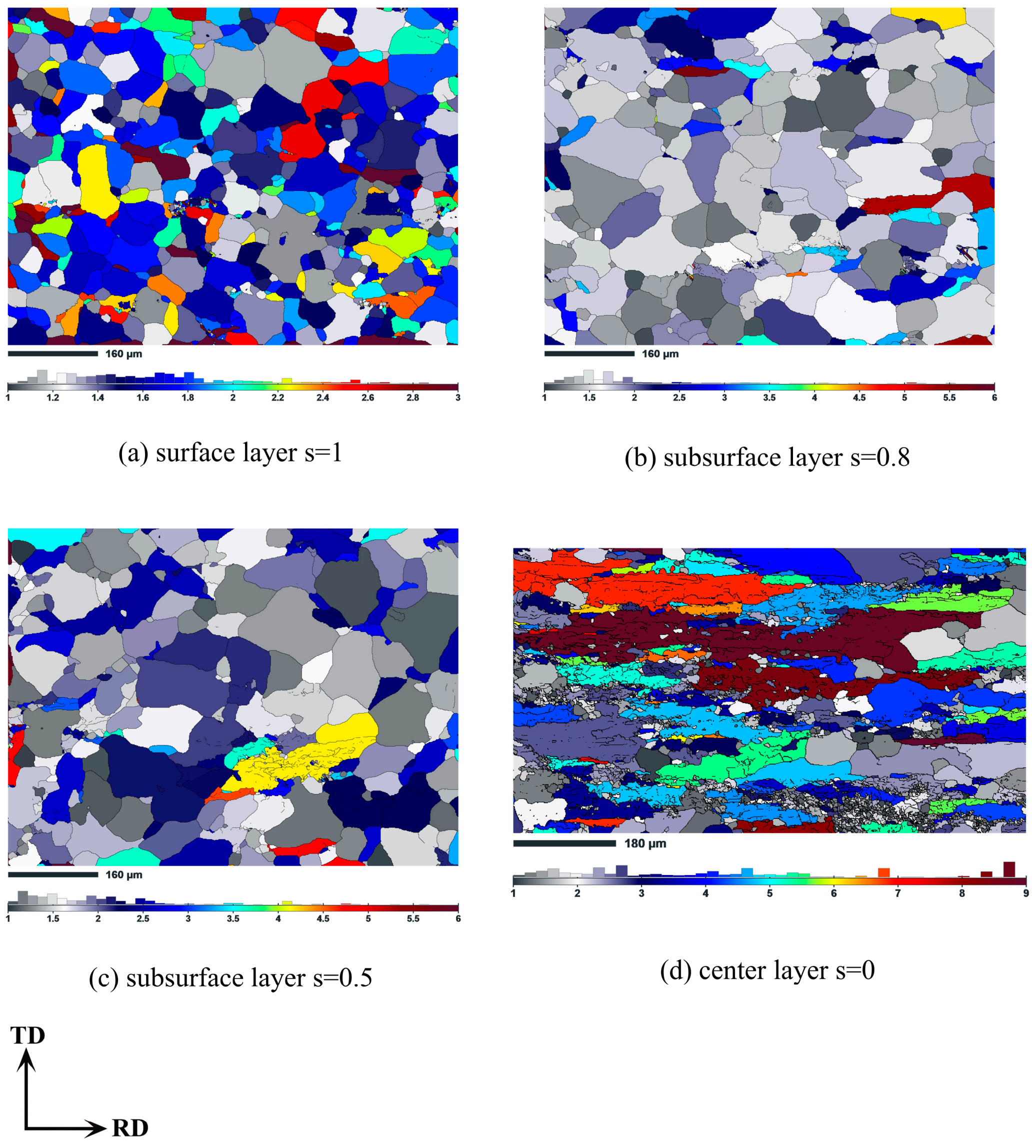

Figure 2. Grain aspect ratio of different layers of hot-rolled plate, (**a**) surface layer s = 1, (**b**) subsurface layer s = 0.8, (**c**) subsurface layer s = 0.5, (**d**) center layer s = 0.

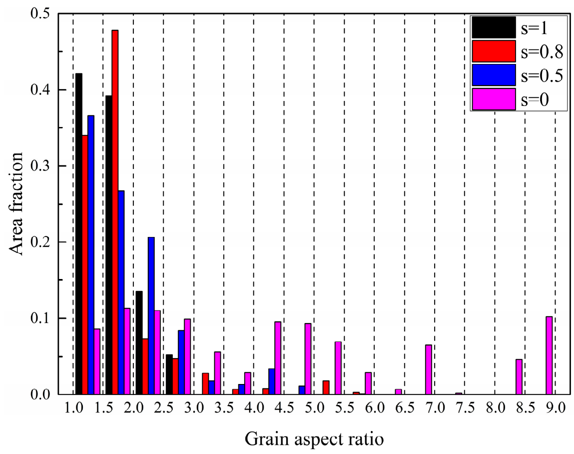

Figure 3. The comparison of the grain aspect ratio between different layers of hot-rolled plate.

3.2. The Texture of Hot-Rolled Plate along the Thickness Direction

Figure 4 shows the typical orientations in the (100) pole figures, and Figure 5 shows the (100) pole figures representing the macro-texture along the thickness direction of hot-rolled plate measured using XRD. The texture of the surface layer s = 1 shows a certain randomness, which is different from that of the subsurface layer s = 0.5~0.9 and center layer s = 0~0.4. Relatively high {112}<111> Cu, {110}<112> (A1 and A2) and {213}<364> (S1 and S2) intensities exist in the subsurface layer s = 0.7~0.9, and relatively high {441}<104> (C1 and C2) and (110)[001] Goss (Gs) intensities exist in the subsurface layer s = 0.5~0.6. However, a typical α-fiber texture exists in the center layer s = 0~0.4, and the α-fiber texture in the center layer s = 0~0.4 is highly concentrated in the {100}<011> RCb orientation, while the {100}<011> RCb intensity rapidly increases along the thickness direction and reaches a peak in the center layer s = 0, which is different from that of the subsurface layer s = 0.5~0.9 and surface layer s = 1.

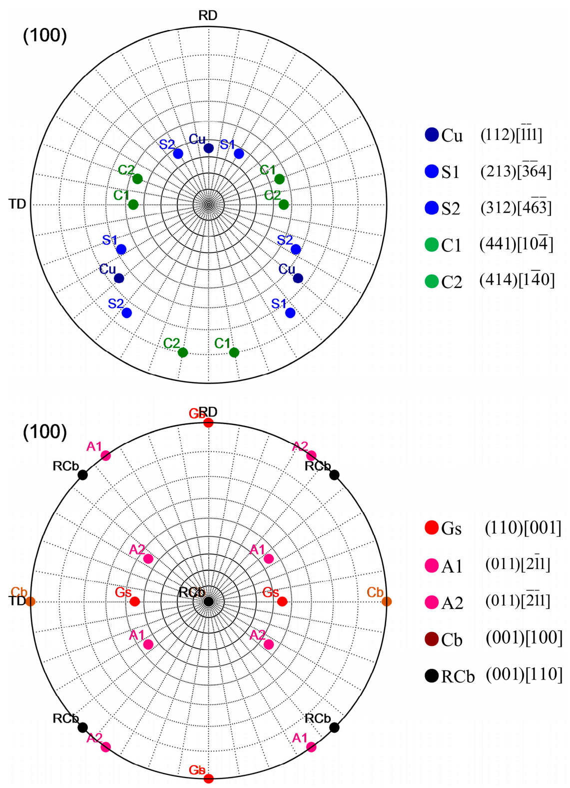

Figure 4. The (100) pole figures representing typical orientations in the hot-rolled plate.

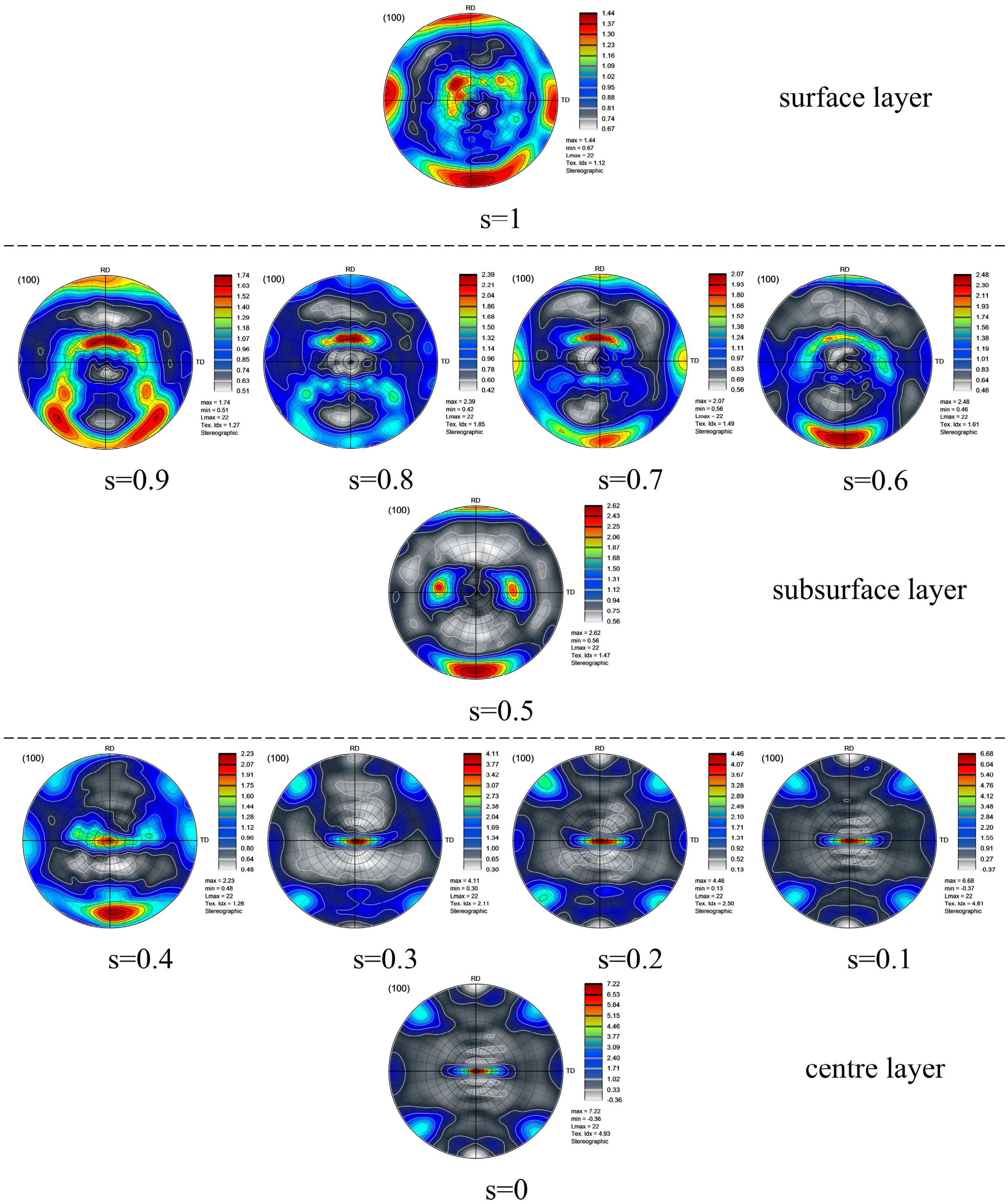

Figure 5. The (100) pole figures representing the texture of hot-rolled plate along the thickness direction.

3.3. Fiber Texture in the Subsurface Layer (s = 0.5~0.9) of Hot-Rolled Plate

Figure 6 shows the ODFs of the subsurface layer s = 0.5~0.9 of hot-rolled plate measured using XRD, and the ODFs of φ2 = 45°, 63°, 72°, 75° and 90° are selected to represent the distribution of the texture. In the subsurface layer s = 0.5~0.9, the texture is continuous in Euler space and highly concentrated in some specific orientations, which can be considered as the formation of fiber texture, and the black frame represents fiber texture in the ODFs. In the subsurface layer (a) s = 0.9, fiber texture starts from the orientation near Cu, crosses through Euler space (φ2 = 45°~90°) and ends in A1 and A2 orientations, respectively. In the subsurface layer (b) s = 0.8, fiber texture becomes more concentrated in Cu, A1 and A2 orientations, and Cu, A1 and A2 intensities reach their maximum values. In the subsurface layer (c) s = 0.7 and (d) s = 0.6, fiber texture gradually deviates from Cu, A1 and A2 orientations and becomes concentrated in S1, S2, C1, C2 and Goss (Gs) orientations.

Finally, in the subsurface layer (e) s = 0.5, fiber texture is highly concentrated in C1, C2 and Goss orientations, and the Goss intensity reaches its maximum value.

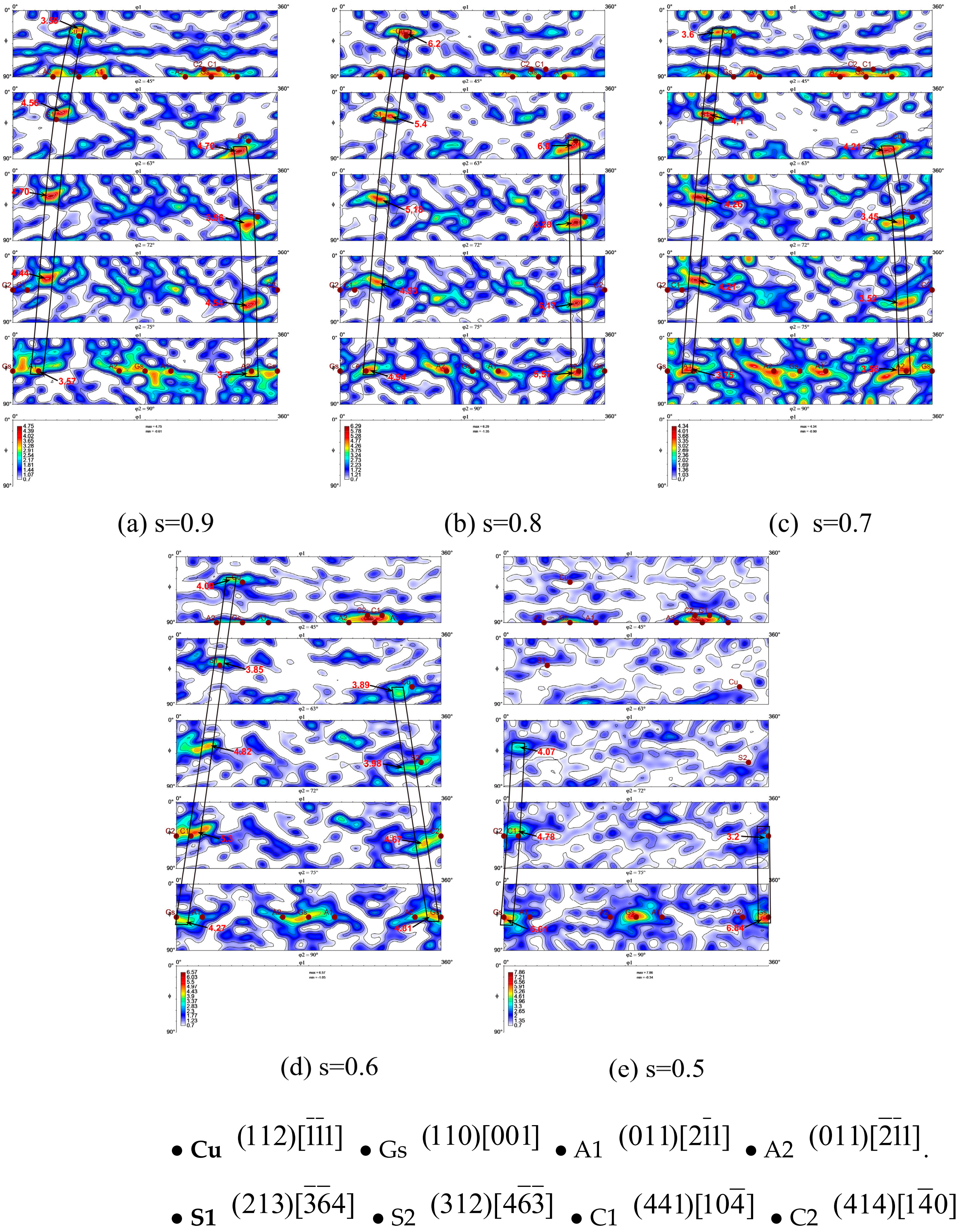

Figure 6. ODFs representing the texture in the subsurface layer s = 0.5~0.9 of hot-rolled plate.

4. Discussion

4.1. The Formation and Evolution of Microstructure in the Hot-Rolled Plate

During high-temperature plastic deformation, under the combination of compressive force and shear force, the nuclei of recrystallized grains were formed through the activities of several specific slip systems. High shear force exists in the surface layer during hot rolling, resulting in a great quantity of intragranular deformation bands and nucleation sites at the grain boundaries, which contributes to the formation of a large number of equiaxed grains in the surface layer s = 1, as shown in Figure 2a. Under the surface layer, shear force decreases along the thickness direction of hot-rolled plate, resulting in a reduction in intragranular deformation bands and nucleation sites at grain boundaries during the hot rolling process. It can be concluded that the reduction in shear force inhibits the formation of equiaxed grains in the subsurface layer and center layer; thus, the shape of the recrystallized grains in the subsurface layer gradually elongates along the rolling direction, and some recrystallized grains in the center layer s = 0 can significantly elongate along the rolling direction, as shown in Figures 2 and 3. In addition, the addition of 3%Si in grain-oriented silicon steel can greatly reduce the recovery rate and recrystallization rate during recrystallization [30]. This leads to a decrease in nucleation rate and recrystallization rate during the recrystallization process, which contributes to the formation of the inhomogeneous microstructure in the hot-rolled plate.

Therefore, along the thickness direction of hot-rolled plate, the decreasing shear force leads to the elongation and irregularity of the recrystallized grains. During hot rolling, the formation of the inhomogeneous microstructure and variations of texture in the hot-rolled plate are determined by the combination of compressive force and shear force applied by the hot roller.

4.2. The Formation and Evolution of Fiber Texture under the Surface Layer of Hot-Rolled Plate

After cold rolling and annealing, the initial orientation of 3%Si iron single crystal was generally changed to another orientation or remained unchanged [31,32], and the texture evolution of single crystal was usually simple. However, the texture evolution of 3%Si iron polycrystal during hot rolling was very intricate; recrystallized grains with dozens of orientations were formed through shear deformation and recrystallization, which led to the formation and evolution of fiber texture in the hot-rolled plate.

During hot rolling, different specific slip systems were activated by the decreasing shear force along the thickness direction. Fiber texture composed of dozens of orientations was formed and gradually evolved along the thickness direction, and the evolution of fiber texture was a gradual process in the subsurface layer s = 0.5~0.9, as shown in Figure 6. However, the evolution of fiber texture composed of dozens of orientations along the thickness direction is too complicated; therefore, the typical orientations of Cu, Gs (Goss), S1, S2, C1, C2 and RCb are selected to illustrate the evolution of fiber texture.

Figures 5 and 6 indicate that the formation of {112}<111> Cu texture is a priority in the subsurface layer s = 0.8~0.9, and Shimizu [33] reported that {112}<111> orientation was formed on the surface of {100}<011> single crystal after hot rolling. Along the thickness direction of hot-rolled plate, {213}<364> (S1 and S2) texture is preferentially formed in the subsurface layer s = 0.7~0.8, {441}<104> (C1 and C2) and (110)[001] Goss texture is preferentially formed in the subsurface layer s = 0.5~0.6 and eventually {100}<011> RCb texture is preferentially formed in the center layer s = 0~0.4. It can be concluded that, under the combination of compressive force and shear force, the evolution of fiber texture along the thickness direction of hot-rolled plate can be represented as Cu→S1→C1→Goss→RCb and Cu→S2→C2→Goss→RCb, as shown in Figure 7.

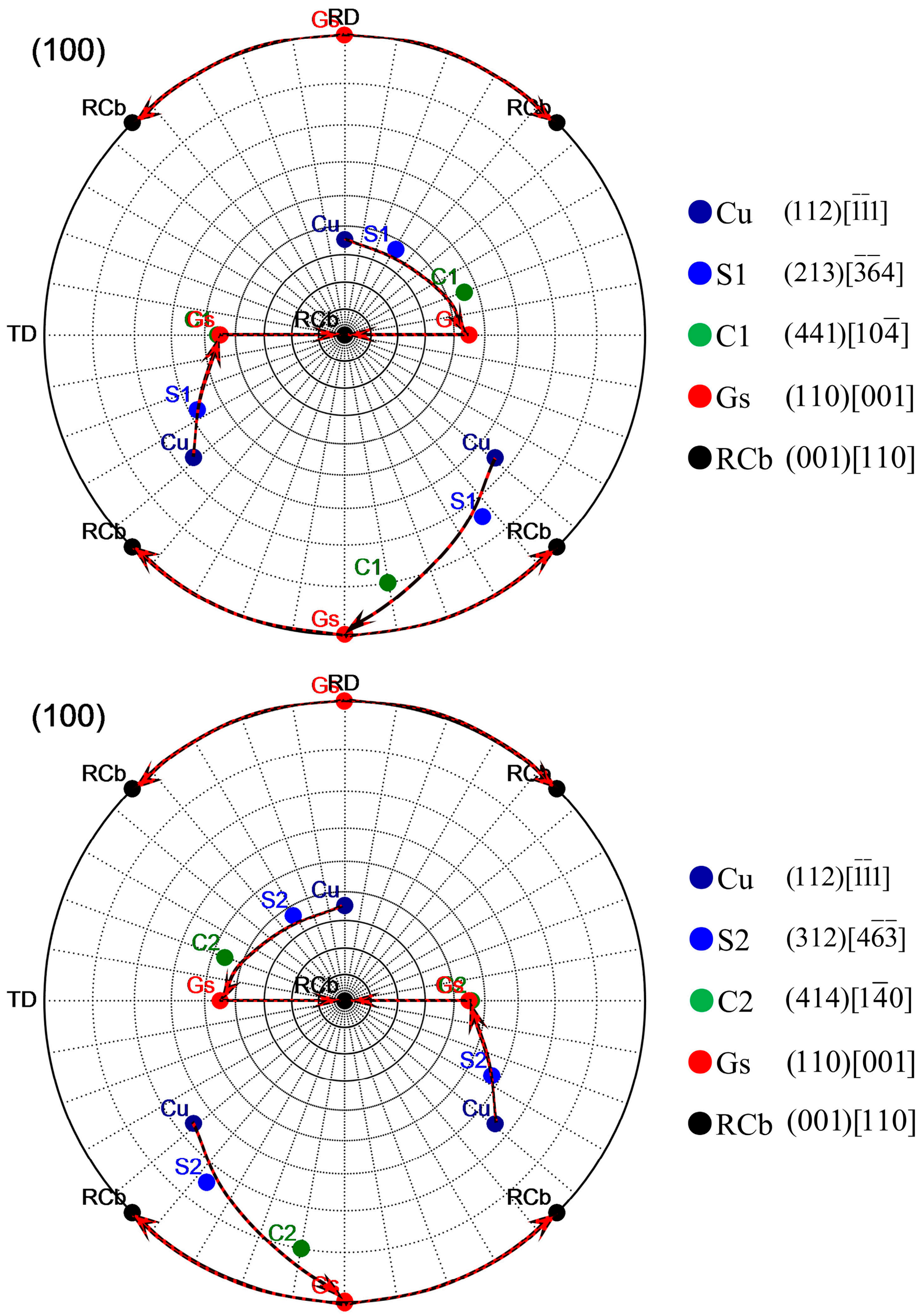

Figure 7. The (100) pole figures representing the evolution of fiber texture along the thickness direction of hot-rolled plate.

Figure 8 shows the schematic of the crystal rotation through the thickness of hot-rolled plate (s = 0~0.9). During high-temperature plastic deformation, {112}<111>, {213}<364>, {441}<104> and Goss-oriented grains were formed in the subsurface layer s = 0.5~0.9 through the combination of compressive force and decreasing shear force. Under the condition of decreasing shear force, recrystallized {112}<111>, {213}<364>, {441}<104> and Goss grains were forced to deform and elongate along the rolling direction instead of through nucleation and recrystallization on the intragranular deformation bands and deformed grain boundaries, which inhibited the formation of equiaxed grains with different orientations in the subsurface layer and led to the formation and evolution of a symmetrical fiber texture (Cu→S1→C1→Goss and Cu→S2→C2→Goss) in the subsurface layer s = 0.5~0.9, as shown in Figures 5 and 6.

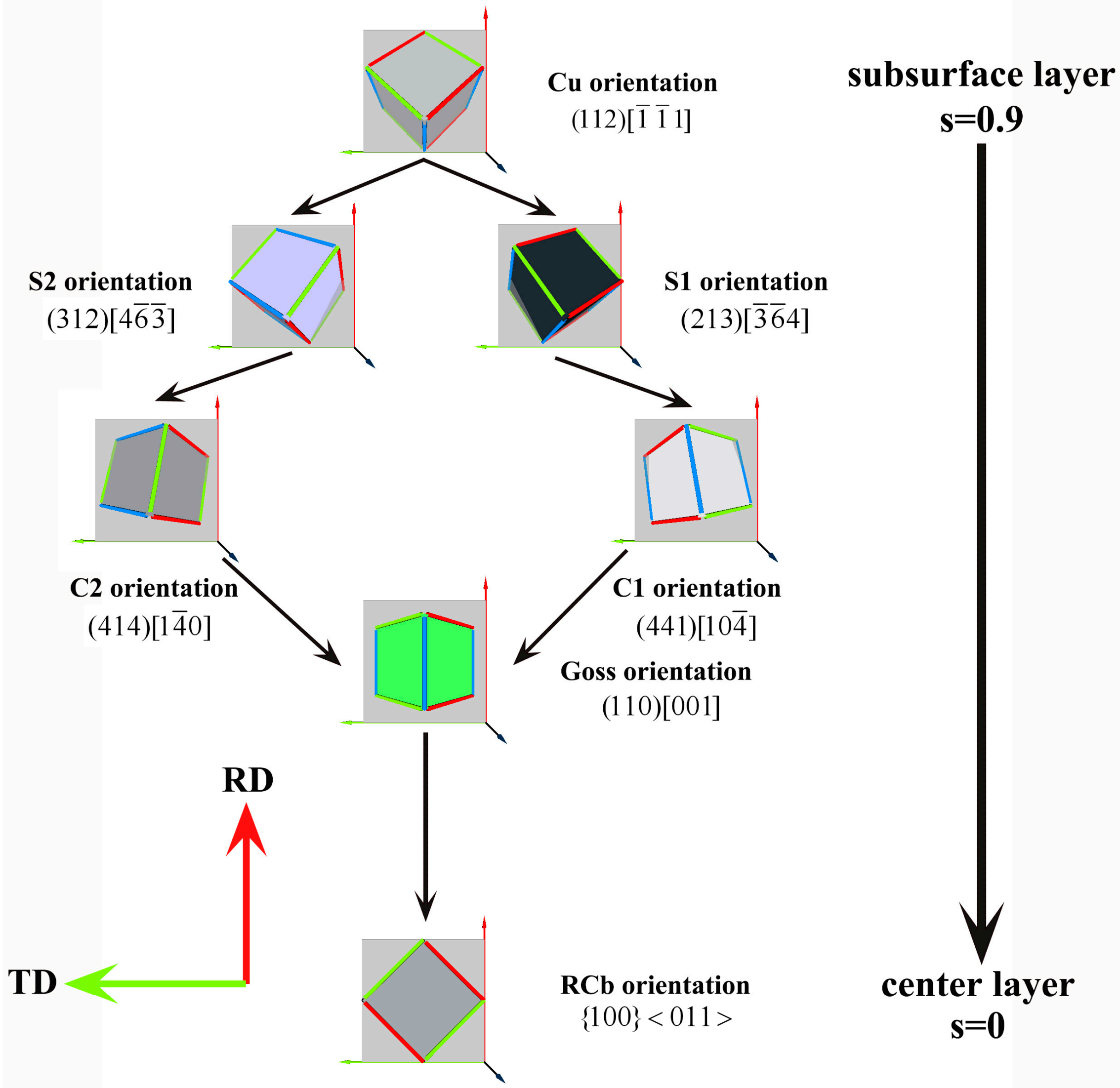

Figure 8. The schematic of crystal rotation through the thickness of hot-rolled plate.

It is concluded that the evolution of fiber texture is formed in the subsurface layer of hot-rolled plate of grain-oriented silicon steel during hot rolling. However, it can be assumed that different materials can form unique fiber textures composed of specific orientations and specific texture evolutions during different hot rolling processes, rather than some random and independent orientations forming during the hot rolling process, which is helpful for studying the texture control of different materials (carbon steel, alloy steel, non-ferrous alloy, etc). In addition, the formation and evolution of the microstructure during hot rolling may be highly correlated with the formation of specific orientations of materials, which can be a meaningful and attractive research subject.

4.3. Effect of Shear Force on the Formation of Goss-Oriented Grains in the Hot-Rolled Plate

During hot rolling, under the combination of compressive force and high shear force, a large number of equiaxed grains were formed in the surface layer s = 1, and the texture of the surface layer showed a certain randomness, as shown in Figure 5. Relatively low Goss intensity exists in the surface layer s = 1, and Goss-oriented grains have no advantage over other oriented grains. Therefore, it can be concluded that, under the condition of high shear force, the formation of a large number of equiaxed grains leads to the formation of random texture, and it is difficult to obtain high-intensity Goss texture and control random texture in the surface layer of hot-rolled plate.

Under the surface layer, fiber texture was formed in the subsurface layer s = 0.5~0.9 of hot-rolled plate. Fiber texture in the subsurface layer s = 0.5 was mainly composed of {441}<104> and (110)[001] Goss texture, as shown in Figure 6. During the formation and evolution of fiber texture, the nuclei of Goss grains were formed through the combination of compressive force and decreasing shear force, and then grew into recrystallized Goss grains. When the recrystallized Goss grains were forced to deform, the formation of equiaxed grains originating from intragranular deformation bands and deformed grain boundaries was greatly inhibited by the decrease in shear force, resulting in the elongation and irregularity of recrystallized Goss grains, as shown in Figure 2c, and eventually contributed to the formation of Goss-oriented grains and highly concentrated Goss texture in the subsurface layer s = 0.5 of hot-rolled plate.

It can be concluded that the formation of Goss texture is only a small part of fiber texture and texture evolution in the subsurface layer of hot-rolled plate, and it is difficult to obtain a large quantity of Goss-oriented grains in the hot-rolled plate. Therefore, the control of shear force is crucial for the formation of the microstructure and texture in the hot-rolled plate. During high-temperature plastic deformation, relatively low shear force contributes to the formation of elongated and irregular recrystallized grains and inhibits the formation of equiaxed grains, which is conducive to the accumulation and improvement of Goss texture in the subsurface layer of hot-rolled plate. On the contrary, relatively high shear force contributes to the increase in the proportion of equiaxed grains in the hot-rolled plate, as a large number of equiaxed grains originating from intragranular deformation bands and deformed grain boundaries are prone to forming under relatively high shear force, which is not conducive to the formation of elongated and irregular recrystallized Goss grains and highly concentrated Goss texture in the subsurface layer.

5. Conclusions

During high-temperature plastic deformation, a large number of equiaxed grains with a random texture are formed in the surface layer s = 1 under the combination of compressive force and high shear force. Under the surface layer, it can be concluded that, along the thickness direction (s = 0~0.9) of hot-rolled plate, the shape of the recrystallized grains gradually elongates along the rolling direction and becomes more irregular along the thickness direction. It can be assumed that the decrease in shear force inhibits the nucleation and growth of equiaxed grains originating from intragranular deformation bands and deformed grain boundaries, and the reduction in shear force inhibits the formation of equiaxed grains along the thickness direction of hot-rolled plate, which leads to the shape of the recrystallized grains gradually elongating along the rolling direction and becoming irregular. During hot rolling, under the combination of compressive force and decreasing shear force along the thickness direction (s = 0~0.9), it can be concluded that fiber texture composed of dozens of specific orientations is formed in the subsurface layer s = 0.5~0.9 of hot-rolled plate, as well as some typical orientations of the fiber texture such as {112}<111> Cu, {213}<364> (S1 and S2), {441}<104> (C1 and C2) and (110)[001] Goss. Fiber texture of the subsurface layer s = 0.5 is mainly composed of {441}<104> and (110)[001] Goss texture, and the formation of highly concentrated Goss texture in the subsurface layer s = 0.5 is only a small part of the fiber texture and texture evolution in the subsurface layer s = 0.5~0.9 of hot-rolled plate. Finally, it can be concluded that the symmetrical evolution of fiber texture (s = 0.5~0.9) along the thickness direction can be represented as Cu→S1→C1→Goss and Cu→S2→C2→Goss.

This study is only a preliminary study on the formation of the microstructure and texture evolution of hot-rolled plate. In future work, the mechanism of grain growth and texture evolution in hot-rolled plate of grain-orientated silicon steel will be the focus of further research.

Author Contributions: Conceptualization, X.Z.; writing—original draft, X.Z.; writing—review and editing, S.Q.; visualization X.Z.; supervision, Q.L.; project administration, Q.L.; funding acquisition, S.Q. All authors have read and agreed to the published version of the manuscript.

Funding: This research received no external funding.

Data Availability Statement: Data are available on request due to restrictions, e.g., privacy or ethical.

Conflicts of Interest: The authors declare no conflict of interest.

References

1. Taguchi, S.; Sakakura, A.; Matsumoto, F.; Takashima, K.; Kuroki, K. The development of grain-oriented silicon steel with high permeability. *J. Magn. Magn. Mater.* **1975**, *2*, 121–131. [CrossRef]
2. Matsuo, M. Texture control in the production of grain oriented silicon steels. *ISIJ Int.* **1989**, *29*, 809–827. [CrossRef]
3. Dunn, C.G. Secondary recrystallization textures and their origin in cold-rolled single crystals of silicon iron. *Acta Metall.* **1953**, *1*, 163–175. [CrossRef]
4. Hayakawa, Y.; Szpunar, J.A. The role of grain boundary character distribution in secondary recrystallization of electrical steels. *Acta Mater.* **1997**, *45*, 1285–1295. [CrossRef]
5. Fang, F.; Wang, J.; Yang, J.; Zhang, Y.; Wang, Y.; Yuan, G.; Zhang, X.; Misra, R.D.K.; Wang, G. Formation of η-oriented shear bands and its significant impact on recrystallization texture in strip-cast electrical steel. *J. Mater. Res. Technol.* **2022**, *21*, 1770–1783. [CrossRef]
6. Lohan, N.M.; Pricop, B.; Popa, M.; Matcovschi, E.; Cimpoesu, N.; Cimpoesu, R.; Istrate, B.; Bujoreanu, L.G. Hot rolling effects on the microstructure and chemical properties of NiTiTa alloys. *J. Mater. Eng. Perform.* **2019**, *28*, 7273–7280. [CrossRef]
7. Birosca, S.; Nadoum, A.; Hawezy, D.; Robinson, F.; Kockelmann, W. Mechanistic approach of Goss abnormal grain growth in electrical steel: Theory and argument. *Acta Metall.* **2020**, *185*, 370–381. [CrossRef]
8. Zhou, M.C.; Zhang, X.F. Regulating the recrystallized grain to induce strong cube texture in oriented silicon steel. *J. Mater. Sci. Technol.* **2022**, *96*, 126–139. [CrossRef]
9. Alves, E.M.M.; Silveira, C.C.; da Cunha, M.A. Influence of stress relief annealing temperature on the cutting edge microstructure and on the recovery of magnetic properties of grain oriented electrical steel. *Mater. Charact.* **2020**, *166*, 110408. [CrossRef]
10. Hashimoto, O. Formation mechanism of Goss texture in hot rolled 3% silicon steel. *Tetsu-to-Hagane* **1988**, *74*, 1633–1640. [CrossRef]
11. Mineo, M.; Tetsuo, T.; Kei, S.; Takashi, O.; Eiichi, F. Formation Mechanism of {111} Recrystallization Texture in Ferritic Steels. *Tetsu-to-Hagane* **1999**, *85*, 751–757. [CrossRef]
12. Mukhopadhyay, A.; Howard, I.C.; Sellars, C.M. Finite element modelling of effects of roll gap geometry in hot rolling. *Mater. Sci. Technol.* **2005**, *21*, 901–911. [CrossRef]
13. Matsuo, M. Origin and development of inhomogeneous structure in rolled steel sheets. *Tetsu-to-Hagane* **1984**, *70*, 2090–2096. [CrossRef]
14. Matsuo, M.; Sakai, T.; Suga, Y. Origin and development of through-the-thickness variations of texture in the processing of grain-oriented silicon steel. *Metal Trans. A* **1986**, *17*, 1313–1322. [CrossRef]
15. Inokuti, Y.; Maeda, C.; Ito, Y. Formation of the Goss texture in grain oriented silicon steel containing a small amount of Molybdenum. *Tetsu-to-Hagane* **1984**, *70*, 2057–2064. [CrossRef]
16. Inokuti, Y. Preferential growth of secondary recrystallized Goss grains during secondary recrystallization annealing in grain oriented silicon steel sheet. *Textures Microstruct.* **1996**, *26*, 413–426. [CrossRef]
17. Lee, S.; Ko, K.J.; Kim, S.J.; Park, J.T. Statistical analysis of EBSD data to predict potential abnormal grain growth in 3.0wt% Si grain-oriented electrical steel. *Mater. Charact.* **2020**, *167*, 110450. [CrossRef]
18. Lee, S.; Ko, H.S.; Han, K.; Kim, S.J. Role of subsurface Goss-oriented grains in abnormal grain growth in Fe-3% Si steel. *Mater. Charact.* **2021**, *180*, 1843–1855. [CrossRef]
19. Fang, F.; Dai, S.F.; Zhang, Y.X.; Wang, Y.; Yuan, G.; Wang, M.T.; Wang, G.D. Role of inhibitor behavior in abnormal growth of Goss grain in grain-oriented silicon steel: Experiments and modeling. *J. Mater. Res. Technol.* **2023**, *24*, 2918–2934. [CrossRef]
20. Song, H.Y.; Wang, Y.P.; Esling, C.; Wang, G.D.; Liu, H.T. The role of grain colony on secondary recrystallization in grain-oriented electrical steel: New insights from an original tracking experiment. *Acta Metall.* **2021**, *206*, 116611. [CrossRef]
21. Bottcher, A.; Lucke, K. Influence of subsurface layers on texture and microstructure development in RGO electrical steel. *Acta Metall.* **1993**, *41*, 2503–2514. [CrossRef]
22. Mishra, S.; Darmann, C.; Lucke, K. On the development of the goss texture in iron-3% silicon. *Acta Metall.* **1984**, *32*, 2185–2201. [CrossRef]
23. Zhang, H.M.; Zhang, C.Y.; Wu, Z.W.; Ren, H.P.; Jin, Z.L.; Xing, L. Study on primary recrystallization behavior of Fe–3%Si–Cu alloy with copper-rich precipitates as main inhibitor. *J. Mater. Res. Technol.* **2022**, *21*, 1843–1855. [CrossRef]
24. Tagashira, K.; Nakae, H. Effects of sulfur on the formation of (110)[001] recrystallization texture of 3.17% Si-Fe alloy steel. *J. Jpn. Inst. Met. Mater.* **1971**, *35*, 683–689. [CrossRef]
25. Inokuti, Y.; Maeda, C.; Tanaka, T. Effect of the surface layer of hot-rolled sheet on secondary recrystallization in grain oriented silicon steel containing Molybdenum. *J. Jpn. Inst. Met.* **1985**, *49*, 417–422. [CrossRef]

26. Inokuti, Y. Development of grain oriented silicon steel containing a small amount of Molybdenum and mechanism of secondary recrystallization with Goss orientation. *Bull. Jpn. Inst. Met.* **1988**, *27*, 250–257. [CrossRef]
27. Inokuti, Y. Mechanism of secondary recrystallization in grain oriented silicon steel. *Tetsu-to-Hagane* **1984**, *70*, 2033–2040. [CrossRef] [PubMed]
28. Jiang, W.N.; Wu, X.L.; Yang, P.; Gu, X.; Xie, Q. Formation of Dynamic Recrystallization Zone and Characteristics of Shear Texture in Surface Layer of Hot-Rolled Silicon Steel. *Acta Metall Sin.* **2022**, *58*, 1545–1556. [CrossRef]
29. Beausir, B.; Fundenberger, J.-J. *Analysis Tools for Electron and X-ray Diffraction, ATEX—Software*; Université de Lorraine: Metz, France, 2017. Available online: www.atex-software.eu (accessed on 30 September 2022).
30. Ahn, Y.K.; Jeong, Y.K.; Kim, T.Y.; Cho, J.U.; Hwang, N.M. Texture evolution of non-oriented electrical steel analyzed by EBSD and in-situ XRD during the phase transformation from γ to α. *Mater. Today Commun.* **2020**, *25*, 101307. [CrossRef]
31. Hashimoto, O.; Ohashi, N.; Fujimoto, K. Studies on the cold rolling and recrystallization textures in single crystal of 3% silicon iron having a <110> rolling direction. *Tetsu-to-Hagané* **1971**, *57*, 1155. [CrossRef]
32. Hashimoto, O.; Ohashi, N.; Fujimoto, K. Formation of 011 <100> primary recrystallization texture in single crystals of ferritic iron alloys having a <110> rolling direction. *Tetsu-to-Hagané* **1971**, *57*, 1167. [CrossRef]
33. Shimizu, Y.; Ito, Y.; Iida, Y. Formation of the Goss orientation near the surface of 3 pct silicon steel during hot rolling. *Metal Trans. A* **1986**, *17*, 1323–1334. [CrossRef]